

# THE 4TH INTERNATIONAL CONFERENCE ON ALUMINUM ALLOYS

## MICROSTRUCTURE AND DEFORMATION BEHAVIOR OF HIGH-TEMPERATURE P/M AL-ALLOYS

O. Roder, J. Albrecht, G. Lütjering  
Technical University Hamburg-Harburg, 21071 Hamburg, Germany

### Abstract

The tensile and fatigue properties of P/M processed Al-alloys containing intermetallic dispersoids were tested in the temperature range of 20°C to 300°C. Three alloys were investigated: one based on the composition Al-10Mn, and two alloys based on Al-Fe with 6 % and 12 % Fe, resp.. To further vary the microstructure, the Al-10Mn alloy was subjected to annealing treatments to coarsen the dispersoids and the grains. The results of the mechanical tests are related to the microstructural parameters: grain size, volume fraction, spacing, and size of the dispersoids.

### Introduction

Aluminum alloys with temperature capabilities above 150°C (up to 300°C) would open opportunities for weight savings in aerospace applications by replacing heavier heat resisting alloys. Conventional high-strength Al-alloys are generally precipitation hardened by aging at temperatures typically below 200°C, which limits the maximum service temperature to about 150°C. Long exposure times during service at temperatures beyond this limit would overage the material and decrease the strength. For higher temperature strength, the strengthening by metastable precipitates has to be replaced by dispersion hardening with thermally stable phases, e.g. intermetallic compounds. To achieve high strength, a small size of the dispersoids in combination with a high volume fraction is mandatory. This condition cannot be met by conventional ingot-metallurgy processing. It requires rapid solidification of melts with appropriate compositions, which can be achieved by powder metallurgical methods, e.g. inert gas atomization or melt spinning (1,2,3). Suitable elements to form stable dispersoids are transition elements, particularly Fe, Mn, Ti and Zr, due to their low solid solubility and their small diffusion coefficient in aluminum. Several commercial alloys of this type were developed in the past years, mainly based on the Al-Fe composition, like Allied-Signals Al-Fe-V-Si alloys (4,5). Similar materials were developed on the basis of Al-Mn (6).

This paper describes the investigation of two alloys of the type Al-Fe-V-Si with different amounts of dispersoids, and one alloy based on the system Al-Mn. Emphasis was on the deformation behavior, particularly at elevated temperature under tensile and fatigue conditions. The results of the mechanical tests are related to the microstructural parameters of the materials.

### Experimental Procedure

Three dispersion strengthened alloys were investigated (compositions in wt.-%): Al-10Mn-1.6Si-4Ti (designation: Al-10Mn), Al-6.5Fe-0.6V-1.3Si (designation Al-6Fe), and Al-11.7Fe-1.2V-2.4Si (designation Al-12Fe). Test material of Al-10Mn was prepared from argon-atomized powders, sieved to a powder fraction of < 36 µm. The powder was canned, cold pressed and

vacuum degassed at 450°C. The sealed can was hot pressed and extruded to a diameter of 14 mm. Alloys Al-6Fe and Al-12Fe were delivered by Allied Signal, Inc., in the form of extruded rods with a diameter of 36 mm or 39 mm, respectively. The material was produced and consolidated by Allied Signal applying their proprietary Planar Flow Casting (PFC) process. All specimens for mechanical testing were machined with the load axis parallel to the extrusion direction. Specimen blanks of alloy Al-10Mn were subjected to additional heat treatments for 48h at 500°C and another series for 96h at 550°C in order to coarsen the dispersoids and the grain size.

Tensile tests were performed in the temperature range of 20°C to 350°C with an initial strain rate of  $\dot{\epsilon} = 6.7 \times 10^{-4} \text{ s}^{-1}$ . In addition, high-speed tensile tests at a strain rate of about  $2.5 \times 10^0 \text{ s}^{-1}$  were done at 20°C and 300°C. For the fatigue tests at 20°C and 300°C at an R-ratio of 0.1, hour-glass shaped specimens with electrolytically polished surfaces were used. The test frequency was about 90 Hz, resulting in a strain rate in the range of  $5\text{-}8 \times 10^{-1} \text{ s}^{-1}$ .

## Results and Discussion

### Microstructure

The microstructure of the three alloys in the as-received condition is shown in the TEM-micrographs Figs. 1-3. Fig. 1 shows the grain structure and the dispersoid distribution of alloy Al-10Mn. The grain size is fairly small, about 0.5  $\mu\text{m}$  with occasional areas of coarser grains up to 1  $\mu\text{m}$ . Two types of dispersoids are observed: larger ones of the type  $\text{Al}_6\text{Mn}$ , located preferentially at grain boundaries and triple points, and finer  $\text{Al}_3\text{Ti}$  dispersoids within the grains. The grain size of Al-6Fe (Fig. 2) is considerably larger (about 2  $\mu\text{m}$ ), but very homogeneous. In particular, areas with a larger grain size were not observed. The dispersoids of the type  $\text{Al}_{13}(\text{Fe},\text{V})_3\text{Si}$  are equally homogeneously distributed. Alloy Al-12Fe shows an inhomogeneous grain structure: areas with a very small grain size of 0.4  $\mu\text{m}$  and a fair amount of coarse grained areas, as shown in Fig. 3. The distribution of the dispersoid is also inhomogeneous, particularly in the coarse grained areas, where clusters of fine dispersoids are observed.

### Tensile Properties

The tensile properties of the three alloys in the as-received condition are shown in Figs. 4a (yield stress) and 4b (ductility) as a function of test temperature for the conventional, low strain rate ( $6.7 \times 10^{-4} \text{ s}^{-1}$ ). At room temperature, alloy Al-12Fe has the highest yield stress (490 MPa), closely followed by Al-10Mn (470 MPa), while the yield stress of Al-6Fe is considerably lower (280 MPa). With increasing test temperature, the yield stress of all three alloys decreases. In comparison with the temperature dependence of Young's Modulus, which is also included in Fig. 4a, the yield stress decreases overproportionally, i.e. the ratio of yield stress to modulus decreases with temperature. The ductility of the three alloys in the as-received condition is shown in Fig. 4b. At room temperature, Al-6Fe has by far the highest ductility (1.3); a value of 0.18 was measured for Al-12Fe and even lower (0.05) for Al-10Mn. The ductility of Al-6Fe decreases with temperature, most pronounced between room temperature and 200°C, while the ductility of Al-12Fe and Al-10Mn remains fairly constant over the whole temperature range.

This temperature dependence cannot be explained by a mechanism of dislocation motion leading to void formation at dispersoids. It is believed, that other deformation mechanisms are thermally activated at higher temperature, most likely grain boundary sliding. Evidence for a time dependent deformation mechanism is shown by the results of the high strain rate tensile test, which are superimposed as data points, connected by thicker lines, in Figs. 4a and 4b. The biggest effect is found for the ductility: at room temperature, the ductility is hardly affected by the strain rate, a large increase of the ductility at high temperature is found for the high strain rate. At this high strain rate, the ductility increases with temperature. A similar result is also observed for the yield stress: no or little change of the room-temperature yield stress, while at high temperature the yield stress increases for the high strain rate (c.f. Fig. 4a). Evidence for grain boundary sliding to be the contributing mechanism at high temperature tensile

deformation is found on the fracture surfaces, shown in Fig. 5 (Al-10Mn), Fig. 6 (Al-6Fe), and Fig. 7 (Al-12Fe). Figures a) show the fracture mode at room temperature for the "normal" strain rate ( $6.7 \times 10^{-4} \text{ s}^{-1}$ ); in all cases, the fracture is of ductile, dimpled nature, i.e. formation of voids at dispersoids. Figures b) show the fracture surfaces of samples broken at 300°C with the same ("normal") strain rate; in all three alloys, contributions of faceted grain boundary fracture are observed, most pronounced for Al-6Fe (Fig. 6b). When the strain rate at 300°C is increased to  $2 \times 10^0 \text{ s}^{-1}$ , the fracture mode changes to ductile dimpled fracture similar to that observed at room temperature, as shown in Figs. 5c, 6c and 7c. It is therefore concluded, that at high temperatures, a mechanism of grain boundary sliding is thermally activated; high strain rates suppress this time-dependent mechanism in favor of deformation by dislocation glide, resulting in void formation at dispersoids and concomitantly higher ductility.

More information about the role of microstructural parameters is derived from the tensile tests performed on coarsened material of Al-10Mn. Fig. 8 shows the microstructure of these conditions in comparison with the as-received condition (Fig. 8a). The heat treatment of 48h 500°C results in a coarsening of both grains and dispersoids (Fig. 8b). This effect is even stronger after annealing at 550°C for 96h (Fig. 8c). The grains have grown to a size of about 2  $\mu\text{m}$ , the dispersoids are located almost exclusively at grain boundaries. The resulting tensile test results are shown in Figs. 9a (yield stress) and 9b (ductility). At room temperature, the yield stress of the condition annealed at 500°C is slightly lower than that of the as-received condition, at higher temperature the difference decreases. The condition annealed at 550°C has a distinctly lower yield stress at room temperature, the difference is still noticeable at 300°C. The effect of the annealing treatments on the ductility is shown in Fig. 9b. In comparison with the as-received material, the ductility of both annealed conditions is lower over the whole temperature range, differences between the two annealed conditions are negligible.

To correlate these findings with the microstructural parameters, the size and the volume fraction of the dispersoids were measured for Al-10Mn in the as-received condition and after annealing at 500°C and 550°C, and for Al-6Fe and Al-12Fe in the as-received condition. The results are shown in Table I. From the measured dispersoid size  $D$  and the volume fraction  $f$ , the effective dispersoid spacing  $d_{\text{eff}}$  was calculated. It is interesting to notice that the annealing treatment at 500°C and 550°C increased the volume fraction of Al-10Mn considerably. With the calculated effective dispersoid spacing, the strengthening contribution  $\Delta\tau$  according to an Orowan mechanism was estimated; the calculated values are between 50 and 80 MPa, as shown in Table I. In comparison with the corresponding yield stress values, it is therefore concluded that the strength of the alloys is not derived from dispersion strengthening, but from the very small grain size. As shown in Fig. 10, a good correlation is given when the yield stress of the three conditions Al-10Mn and of Al-6Fe and Al-12Fe is plotted against the inverse square root of the grain size.

The results of tensile tests indicate, that the ductility of these materials is mainly controlled by the volume fraction of the dispersoids. As shown in Fig. 11, where the room temperature ductility of the conditions investigated is plotted against the volume fraction of dispersoids, the ductility decreases with increasing volume fraction of dispersoids, as expected for a type of fracture controlled by void formation at dispersoids.

#### Fatigue properties

The S-N curves of the three alloys in the as-received condition are shown in Fig. 12a (room-temperature) and Fig. 12b (300°C). At both test temperatures, the fatigue strength of Al-10Mn and Al-12Fe is nearly identical (350 MPa at RT and about 200 MPa at 300°C). Alloy Al-6Fe has at both temperatures a distinctly lower fatigue strength (280 MPa at RT and 145 MPa at 300°C). The results indicate, that the fatigue strength of these alloys is mainly controlled by the yield stress, as shown in Table II. Considering the strain rate in a fatigue test at about 90 Hz, it seems appropriate to relate the fatigue strength to the yield stress measured in the high strain rate test. At 300°C, the ratio of fatigue strength to yield strength is nearly the same (0.5 - 0.6), indicating

that at this temperature the yield stress is the dominating parameter. At room temperature, alloy Al-6Fe has a distinctly higher ratio (0.96) than both Al-10Mn (0.77) and Al-12Fe (0.65). This reflects an additional influence of the grain size distribution, which was described above. Alloy Al-6Fe has a large grain size, which results in a low yield stress, but it does not contain coarse grained areas, therefore the ratio of fatigue strength to yield stress is high. The appearance of coarse grained areas even in small concentrations, as found in both Al-10Mn and Al-12Fe, have a detrimental effect on fatigue strength, particularly at low temperatures.

### Conclusion

Some general conclusions can be drawn from the investigation of the tensile and fatigue properties of three P/M processed Al-alloys based on Al-Mn (Al-10Mn) and Al-Fe (Al-6Fe and Al-12Fe):

- The yield stress of these alloys is mainly controlled by the grain size; The very small grain size of 0.5  $\mu\text{m}$  in Al-10Mn and Al-12Fe results in a room temperature yield stress of nearly 500 MPa. The calculated contribution of a strengthening mechanism of bypassing of dispersoids (Orowan-mechanism) were found to be small ( $\Delta\tau = 50\text{-}80$  MPa) in comparison with the yield stress. At high temperatures and "normal" strain rate ( $10^{-4}$  range), thermally activated grain boundary sliding contributes to the deformation.
- The ductility of the alloy is mainly a result of the volume fraction of dispersoids; the ductility relates inversely to the total volume fraction of dispersoids. The abnormal temperature dependence of the ductility results from grain boundary sliding at high temperatures; this mechanism is suppressed at high strain rates, resulting in a ductility increasing with temperature.
- The fatigue strength is primarily controlled by the yield stress of the material. The appearance of coarse grained areas, as observed in Al-10Mn and Al-12Fe, has a negative influence on the fatigue strength. This influence of the grain size distribution decreases with increasing temperature.

### Acknowledgement

This work was supported by the Deutsche Forschungsgemeinschaft (DFG).

### References

1. J. Wadsworth, F.H. Froes: JOM, May 1989, p.12
2. F.H. Froes: Advances in Light-Weight Materials, in: "Space Age Metals Technology", vol. 2, F.H. Froes and P.A. Cull, Eds., SAMPE, Covina, CA (1988), p.1
3. E.A. Starke, J.A. Wert: The Strengthening Mechanisms of Aluminum Powder Alloys in: "High Strength Powder Metallurgy Alloys II", G.J. Hildeman and M.J. Koczak, Eds., TMS, Warrendale, PA (1986), p.3
4. D.J. Skinner, K. Okazaki, C.M. Adam: Physical Metallurgy and Mechanical Properties of Aluminum Alloys Containing Eight to Twelve Percent Iron, in: "Rapidly Solidified Powder Aluminum Alloys", ASTM STP 890, M.E. Fine, E.A. Starke, Jr., Eds., ASTM, Philadelphia, PA (1986), p.211
5. D.J. Skinner et al.: Scripta Met. Vol.20 (1986), p.867
6. B. Saal et al.: A P/M Aluminum Alloy for High-Temperature Application, in "Light Weight Alloys for Aerospace Applications", E.W. Lee, E.H. Chia, N.J. Kim, Eds., TMS, Warrendale, PA (1989), p.3

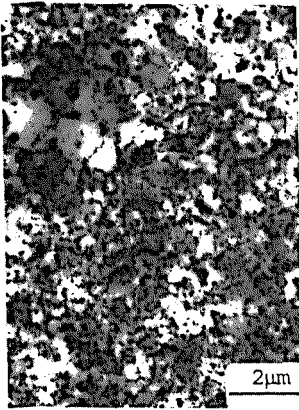


Fig. 1: Microstructure (TEM) of Al-10Mn

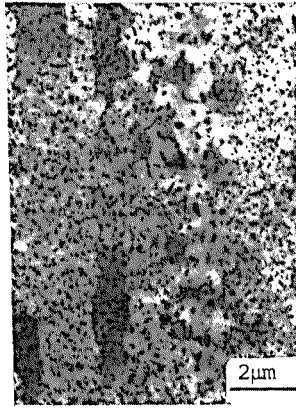


Fig. 2: Microstructure (TEM) of Al-6Fe

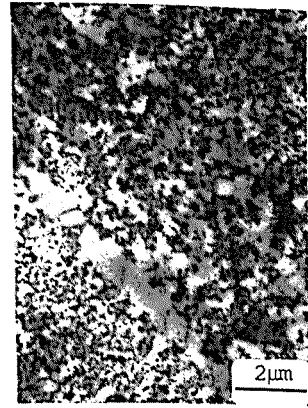
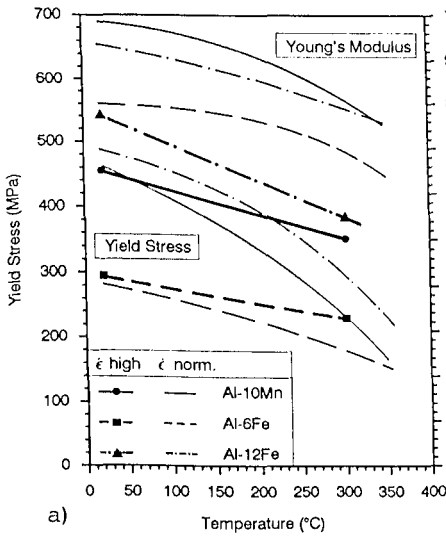
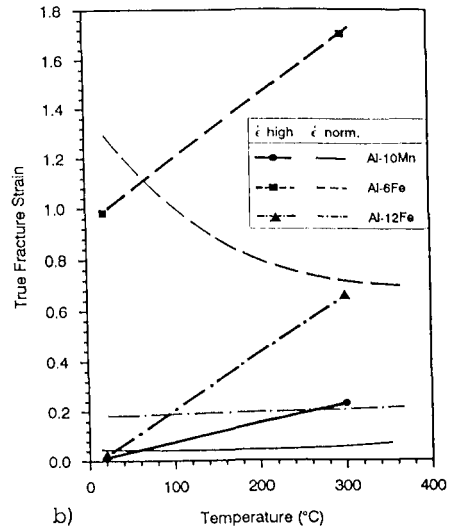


Fig. 3: Microstructure (TEM) of Al-12Fe



a)



b)

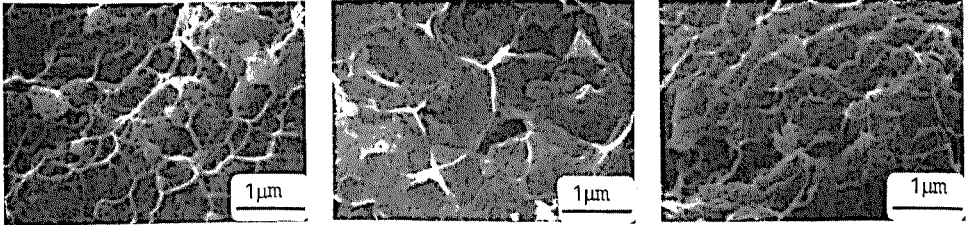
Fig. 4: Tensile properties as a function of test temperature

a) Yield stress and Young's Modulus

b) Ductility

Thin lines: normal strain rate ( $6.7 \times 10^{-4} \text{ s}^{-1}$ )

Data points and thicker lines: high strain rate ( $2 \times 10^0 \text{ s}^{-1}$ )

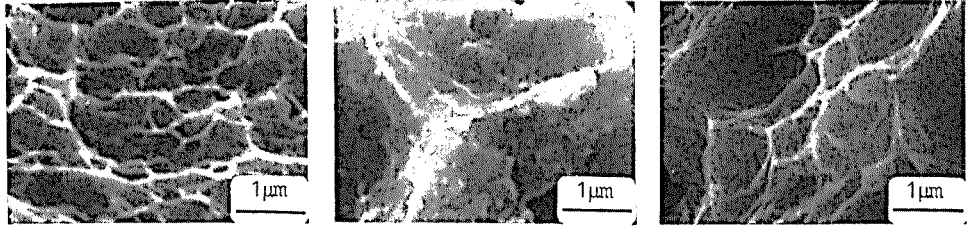


a) RT,  $\dot{\epsilon}$  normal

b) 300°C,  $\dot{\epsilon}$  normal

c) 300°C,  $\dot{\epsilon}$  high

Fig. 5: Fracture surfaces (tensile test) of Al-10Mn

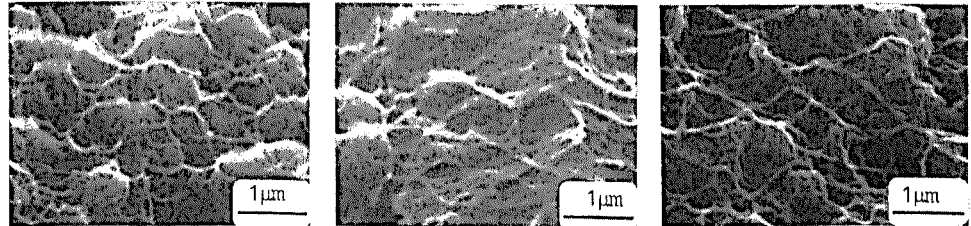


a) RT,  $\dot{\epsilon}$  normal

b) 300°C,  $\dot{\epsilon}$  normal

c) 300°C,  $\dot{\epsilon}$  high

Fig. 6: Fracture surfaces (tensile tests) of Al-6Fe

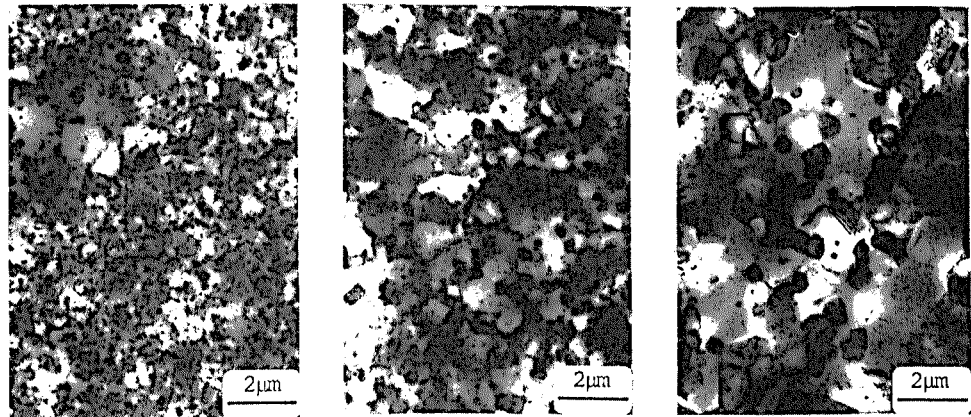


a) RT,  $\dot{\epsilon}$  normal

b) 300°C,  $\dot{\epsilon}$  normal

c) 300°C,  $\dot{\epsilon}$  high

Fig. 7: Fracture surfaces (tensile tests) of Al-12Fe



a) as-received

b) 48h 500°C

c) 96h 550°C

Fig. 8: Microstructure (TEM) of Al-10Mn

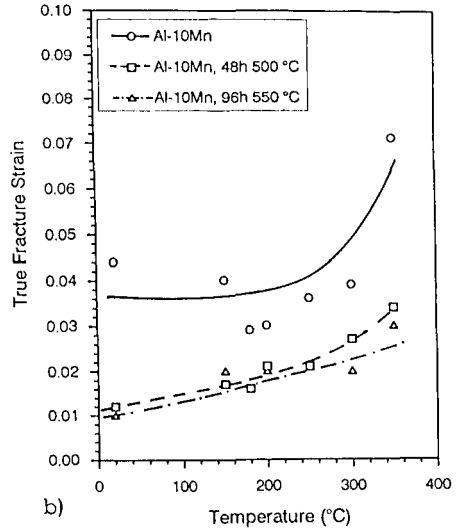
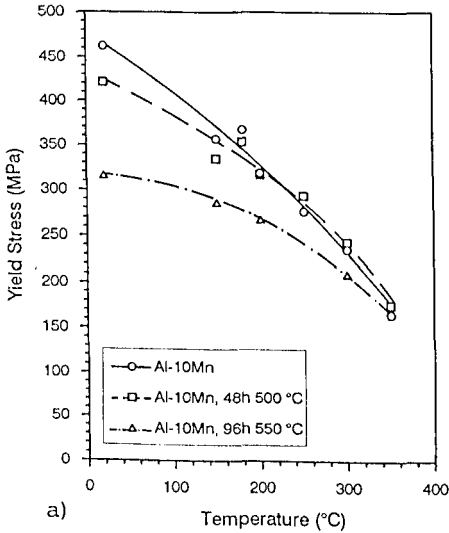


Fig. 9: Tensile properties of Al-10Mn, as-received condition and annealed conditions  
 a) Yield stress  
 b) Ductility

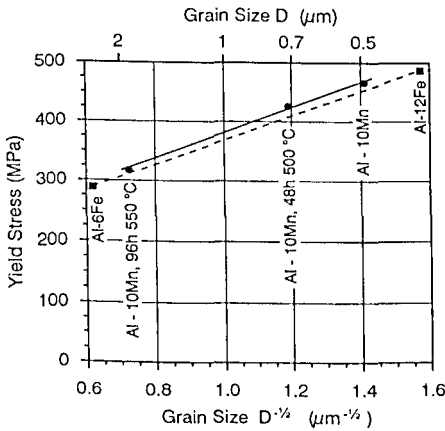


Fig. 10: Yield stress (RT) as function of grain size

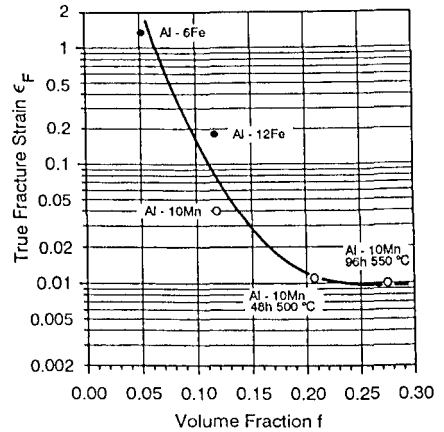


Fig. 11: Ductility (RT) as a function of the volume fraction of dispersoids

Table I: Microstructural parameters and resulting calculated contribution to strength (Orowan)

Condition	D (μm)	f (%)	d <sub>eff.</sub> (μm)	Δτ (MPa)	σ <sub>0.2</sub> (MPa)
Al-10Mn	0.084	0.12	0.108	75	462
Al-10Mn, 48h 500 °C	0.171	0.21	0.132	69	421
Al-10Mn, 96h 550 °C	0.384	0.28	0.216	48	316
Al-6Fe	0.051	0.05	0.120	49	283
Al-12Fe	0.069	0.12	0.101	82	488

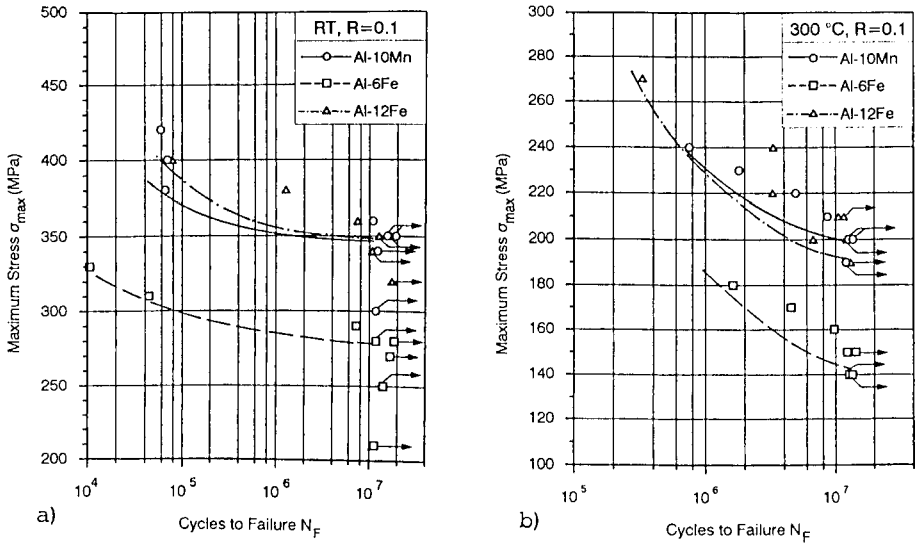


Fig. 12: Fatigue properties at RT (a) and 300°C (b)

Table II: Fatigue strength, yield stress and ratio of fatigue strength to yield stress

Temp. (°C)	Condition	$\sigma_{0.2}$ (MPa)		$\sigma_{max}$ (MPa)	$\sigma_{max}/\sigma_{0.2}$	
		$\epsilon'$ normal	$\epsilon'$ high		$\epsilon'$ normal	$\epsilon'$ high
20	Al-10Mn	462	454	350	0.76	0.77
	Al-6Fe	283	293	280	0.99	0.96
	Al-12Fe	488	542	350	0.72	0.65
300	Al-10Mn	236	351	200	0.85	0.57
	Al-6Fe	181	229	145	0.80	0.63
	Al-12Fe	288	385	190	0.66	0.49